Operator-based linearization for efficient modeling of geothermal processes

Khait, Mark; Voskov, Denis

DOI
10.1016/j.geothermics.2018.01.012

Publication date
2018

Document Version
Final published version

Published in
Geothermics

Geothermics 74 (2018) 7–18

Contents lists available at ScienceDirect

Geothermics

journal homepage: www.elsevier.com/locate/geothermics

Operator-based linearization for efficient modeling of geothermal processes

Mark Khait, Denis Voskov*

Stevinweg 1, 2628 CN Delft, Netherlands

ARTICLE INFO

Keywords:
Geothermal simulation
Coarsening in physical representation
Operator-based linearization

ABSTRACT

Numerical simulation is one of the most important tools required for financial and operational management of geothermal reservoirs. The modern geothermal industry is challenged to run large ensembles of numerical models for uncertainty analysis, causing simulation performance to become a critical issue. Geothermal reservoir modeling requires the solution of governing equations describing the conservation of mass and energy. The robust, accurate and computationally efficient implementation of this solution suggests an implicit time-approximation scheme, which introduces nonlinearity into the system of equations to be solved. The most commonly used approach to solving the system of nonlinear equations is based on Newton's method and involves linearization with respect to nonlinear unknowns. This stage is the most complicated for implementation and usually becomes the source of various errors. A new linearization approach – operator-based linearization – was recently proposed for non-isothermal flow and transport. The governing equations, discretized in space and time, were transformed to the operator form where each term of the equation was specified as the product of two operators. The first operator comprises physical properties of rock and fluids, such as density or viscosity, which depend only on the current state of a grid block, fully defined by the values of nonlinear unknowns. The second operator includes all terms that were not included in the first operators, and depends on both the state and spatial position of a control volume. Next, the first type of operators was parametrized over the physical space of a simulation problem. The representation of highly nonlinear physics was achieved by using multi-linear interpolation, which replaces the continuous representation of parametrized operators. The linearization of the second type of operators was applied in the conventional manner. In this work, we investigated the applicability of this approach to the geothermal processes, specifically for low-enthalpy and high-enthalpy geothermal doublet models with hydrocarbon co-production. The performance and robustness of the new method were tested against the conventional approach on a geothermal reservoir of practical interest. This approach shows significant improvement of geothermal simulation performance, while errors, introduced by coarsening in physics, remain under control. The simplicity of implementation on emerging computational architectures and nonlinearity reduction provide advanced opportunities for uncertainty quantification and risk analysis of geothermal projects.

1. Introduction

The modern development of geothermal resources requires high-performance numerical reservoir simulations. Numerical models are used to predict and compare the performance of different reservoir-development schemes, defined by, e.g., the lifetime of a geothermal doublet in the case of low-enthalpy reservoirs or the recovery of a geothermal reservoir. Complex and fine-scale models enhance prediction accuracy but demand more computational resources. Large ensembles of reservoir models are run to perform sensitivity analysis and reduce uncertainties in parameters estimation. The quality of these processes depends on the number of models in ensembles, which is limited by the computational time required for a single model. Therefore, efficient reservoir simulation performance is essential for geothermal industry: any noticeable improvement could positively affect production workflow.

Numerical geothermal reservoir simulation requires discretization of governing Partial Differential equations (PDE), which describe mass and energy transport in a reservoir. The combination of Finite Volume discretization in space and Fully Implicit Method (FIM) approximation in time provides a robust, accurate and efficient modeling approach (Aziz and Settari, 1979). However, an implicit nature of the time approximation increases the nonlinearity of the governing equations. For those geothermal models that use both gas and liquid phases, complex multiphase behavior and the assumption of thermodynamic equilibrium further amplify nonlinearity.

* Corresponding author.
E-mail address: d.v.voskov@tudelft.nl (D. Voskov).

https://doi.org/10.1016/j.geothermics.2018.01.012
Received 7 July 2016; Received in revised form 11 January 2018; Accepted 30 January 2018

In reservoir simulation, Newton-Raphson's method has become a standard solution for solving the nonlinear system of equations by linearizing it. The linearization is one of the most important and challenging components of a reservoir simulation framework. This step requires the determination of the derivatives of all residual equations with respect to independent variables. The particular set of independent variables (i.e., nonlinear unknowns) is defined by a nonlinear formulation. The flexibility of linearization reflects the simplicity of changing the nonlinear formulation in an existing simulation framework. Based on the formulation, all properties and their derivatives need to be determined and assembled into the matrix of partial derivatives (Jacobian). The linearization stage defines the accuracy and robustness of nonlinear solution, dictates the data layout of a linear system and therefore has a great impact on the reservoir simulation performance.

There are three most commonly used linearization approaches. The first one, numerical derivatives, provides flexibility in the implementation (see Pruess, 2006 for example), but usually lacks robustness (Vanden and Orkwis, 1996) and may lead to a stalled behavior in some cases (O'Sullivan et al., 2014). The second one, straightforward analytical derivations, requires fixing the nonlinear formulation and physical models used in a computational framework and that often limits its flexibility (e.g Geoquest, 2011). Finally, Automatic Differentiation (AD) technique provides both flexibility and robustness to the development of simulators. In reservoir simulation, an Automatic Differentiation General Purpose Research Simulator (ADGPRS) was developed for simulation of generic thermal-compositional problems (Voskov and Tchelepi, 2012; Zaydullin et al., 2014). ADGPRS is a unified reservoir simulation framework providing an extensive set of nonlinear formulations (Voskov, 2011; Zaydullin et al., 2013), including different formulations for a geothermal model (Wong et al., 2015; Wong et al., 2016) and a generic treatment of complex phase behavior (Iranshahr et al., 2010; Iranshahr et al., 2013). Unfortunately, the AD technique by design inherits computational overhead and therefore decreases reservoir simulation performance. Thereby, there is a clear demand for robust, flexible and computationally efficient linearization approach.

A new operator-based linearization (OBL) approach was recently introduced by Voskov (2017). It suggests a different way of linearization, making use of the discrete representation of the physics. In the governing PDE, discretized in time and space, the terms which depend only on state variables are approximated by piece-wise multilinear operators. For a given problem, the current physical state fully defines operators. Therefore, each operator can be parametrized over the multidimensional space of nonlinear unknowns for a given distribution of supporting points, resulting a set of tables. In the course of a simulation, the values of the operators, as well as partial derivatives with respect to nonlinear unknowns, are obtained from the tables using multilinear interpolation. Being as flexible as numerical derivatives, OBL is more consistent and reliable, since the operators are piecewise multilinear functions with derivatives related to the interpolation coefficients. Thus the proposed approach always provides an accurate Jacobian, avoiding stalled behavior and instabilities, which may occur due to the application of numerical derivatives (e.g. challenges in THOUGH2 simulation described by Vanden and Orkwis, 1996; Noy et al., 2012). In addition, it reduces the level of nonlinearity of the problem to be solved, providing a significant improvement in nonlinear solver performance.

In the original approach of Voskov (2017), OBL was described and applied to isothermal hydrocarbon systems. The version of the OBL approach with adaptive parametrization of physical operators was implemented in the ADGPRS framework and tested for petroleum applications in Khait and Voskov (2017a). A special version of a stand-alone isothermal prototype with a limited number of components was implemented in both CPU and GPU architectures in Khait and Voskov (2017b). Here, we farther extend the new prototype framework to thermal systems and investigate an applicability of the OBL method to simulation of geothermal processes, including low-enthalpy and high-enthalpy systems with hydrocarbon co-production. First, we briefly describe the modeling approach. Next, we apply OBL to a realistic geothermal reservoir and compare the performance and solution accuracy against the conventional approach, implemented in ADGPRS. The new simulation prototype demonstrates better performance of simulations with discrete representation of physics where the resolution of interpolation tables controls an approximation error. The proposed simulation framework becomes the essential tool for uncertainty quantification and risk analysis where the performance of forward simulation is the major limiting factor.

2. Modeling approach

Here we describe the state-of-the-art modeling approach of a non-isothermal multiphase multicomponent flow, which was used as a reference solution, followed by the description of operator-based linearization (OBL).

2.1. Conventional modeling approach for thermal compositional problem

This section contains the description of a thermal multiphase compositional problem with n_p phases and n_c components. This problem can be described by n_c equations of mass conservation and one energy equation:

$$\frac{\partial}{\partial t}\left(\phi \sum_{j=1}^{n_p} x_{cj}\rho_j s_j\right) - \operatorname{div}\sum_{j=1}^{n_p} x_{cj}\rho_j\left(K\frac{k_{rj}}{\mu_j}(\nabla p_j - \gamma_j \nabla D)\right) \quad c = 1,\ldots,n_c + \sum_{j=1}^{n_p} x_{cj}\rho_j \tilde{q}_j = 0, \tag{1}$$

$$\frac{\partial}{\partial t}\left(\phi\sum_{j=1}^{n_p}\rho_j s_j U_j + (1-\phi)U_r\right) - \operatorname{div}\sum_{j=1}^{n_p} h_j\rho_j\left(K\frac{k_{rj}}{\mu_j}(\nabla p_j - \gamma_j\nabla D)\right) + \operatorname{div}(\kappa\nabla T) + \sum_{j=1}^{n_p} h_j\rho_j\tilde{q}_j = 0, \tag{2}$$

where:

- ϕ – porosity,
- x_{cj} – the mole fraction of component c in phase j,
- s_j – phase saturations,
- ρ_j – phase molar density,
- K – permeability tensor,
- k_{rj} – relative permeability,
- μ_j – phase viscosity,
- p_j – pressure in phase j,
- γ_j – gravity vector,
- D – depth (backward oriented).
- U_j – phase internal energy,
- U_r – rock internal energy,
- h_j – phase enthalpy,
- κ – thermal conduction.

Next, a finite-volume discretization on a general unstructured mesh and backward Euler approximation in time are applied:

$$V\left[\left(\phi\sum_{j=1}^{n_p} x_{cj}\rho_j s_j\right)^{n+1} - \left(\phi\sum_{j=1}^{n_p} x_{cj}\rho_j s_j\right)^{n}\right] \quad c = 1,\ldots,n_c - \Delta t\sum_{l}\left(\sum_{j=1}^{n_p} x_{cj}^{l}\rho_j^{l}\Gamma_j^{l}\Delta\psi^{l}\right) + \Delta t\sum_{j=1}^{n_p}\rho_p x_{cj} q_j = 0, \tag{3}$$

$$V\left[\left(\phi\sum_{j=1}^{n_p}\rho_j s_j U_j + (1-\phi)U_r\right)^{n+1} - \left(\phi\sum_{j=1}^{n_p}\rho_j s_j U_j + (1-\phi)U_r\right)^{n}\right] - \Delta t\sum_l\left(\sum_{j=1}^{n_p} h_j^l\rho_j^l\Gamma_j^l\Delta\psi^l + \Gamma_c^l\Delta T^l\right) + \Delta t\sum_{j=1}^{n_p} h_j\rho_j q_j = 0 \quad (4)$$

where V is a control volume and $q_j = \tilde{q}_j V$ is a source of phase j. For simplicity, we neglect both gravity and capillarity in the equations above. Here a Two-Point Flux Approximation (TPFA) is applied with an upstream weighting. Based on these simplifications, $\Delta\psi^l$ becomes a simple difference in pressures between blocks connected via interface l, while ΔT^l is a temperature difference between those blocks; $\Gamma_j^l = \Gamma^l k_{rj}^l/\mu_j^l$ is a phase transmissibility, where Γ^l is a constant geometrical part of transmissibility (which involves permeability and the geometry of the control volume). Finally, $\Gamma_c^l = \Gamma^l\kappa = \phi\left(\sum_{j=1}^{n_p} s_j^l\lambda_j^l - \kappa_r\right) + \kappa_r$ is a thermal transmissibility.

Eqs. (3) and (4) are approximated in time using a Fully Implicit Method (FIM). This suggests that convective flux terms $x_{cj}^l\rho_j^l\Gamma_j^l\Delta\psi^l$ for mass and $h_j^l\rho_j^l\Gamma_j^l\Delta\psi^l$ for energy equation as well as the conductive flux $\Gamma_c^l\Delta T^l$ have to be chosen based on values of nonlinear unknowns at the current time step, introducing additional nonlinearities in flux. Also, the closure assumption of instantaneous thermodynamic equilibrium (equality of chemical potentials) further amplifies nonlinearities.

An overall molar formulation (Collins et al., 1992) was chosen among different nonlinear formulations. In this formulation, thermodynamic equilibrium is required at every nonlinear iteration. Hence, the following system must be solved at any grid block contained a multiphase (n_p) multicomponent (n_c) mixture:

$$F_c = z_c - \sum_{j=1}^{n_p}\nu_j x_{cj} = 0, \quad (5)$$

$$F_{c+n_c} = f_{c1}(p, T, x_1) - f_{cj}(p, T, x_j) = 0, \quad (6)$$

$$F_{j+n_c\times n_p} = \sum_{c=1}^{n_c}(x_{c1} - x_{cj}) = 0, \quad (7)$$

$$F_{n_p+n_c\times n_p} = \sum_{j=1}^{n_p}\nu_j - 1 = 0. \quad (8)$$

This procedure, also known as a multiphase flash (Lucia et al., 2000), obtains the phase compositions of a mixture at a given state. Here $z_c = \sum_{j=1}^{n_p} x_{cj}\rho_j s_j/\sum_{j=1}^{n_p}\rho_j s_j$ is the overall composition (i.e., overall mass fraction), $f_{cj}(p, T, x_{cj})$ is the fugacity of component c in phase j and $\nu_j = \rho_j s_j/\sum_j \rho_j s_j$ is the mass fraction of the phase. The multiphase flash solution provides the values of x_{cj} and ν_j. In the molar formulation, the unknowns are p, z_c and T (or h). The physical state ω is completely defined by these variables. As soon as we obtain the solution of multiphase flash, we can determine all derivatives with respect to nonlinear unknowns using the inverse theorem (see Voskov and Tchelepi, 2012, for details).

The conventional linearization approach for the resulting system of nonlinear equations is based on the Newton-Raphson method, which solves on each nonlinear iteration a linear system of equations in the following form:

$$J(\omega^k)(\omega^{k+1} - \omega^k) + r(\omega^k) = 0, \quad (9)$$

where J is the Jacobian defined at a nonlinear iteration k. The conventional approach assumes an accurate numerical representation of properties and their derivatives with respect to nonlinear unknowns. This may demand either various interpolations (for properties such as relative permeabilities) or solution of a highly nonlinear system in combination with chain rule and inverse theorem. As a result, the nonlinear solver has to resolve all small variations in property descriptions, which are sometimes unimportant due to the numerical nature and uncertainties in property evaluation.

2.2. Operator-based linearization approach

Following the OBL approach (Voskov, 2017), all variables in the Eqs. (3) and (4), excluding ones from phase source term, were introduced as functions of a physical state ω and/or a spatial coordinate ξ. We applied several simplifications and assumptions. First, porosity was considered as a pseudo-physical state variable. This step not only allowed to reduce the number of state-dependent operators but also provided a way to extend the compositional model to systems with precipitation and dissolution of solid phase(s). Second, the rock internal energy and thermal conduction were assumed to be spatially homogeneous. These premises were expressed as following:

$$V = V(\xi)\ ;\ \phi\in\omega\ ;\ x_{cj} = x_{cj}(\omega);\ \rho_j = \rho_j(\omega);\ s_j = s_j(\omega); \quad (10)$$

$$x_{cj}^l = x_{cj}^l(\omega_{up})\ ;\ \rho_j^l = \rho_j^l(\omega_{up})\ ;\ k_{rj}^l = k_{rj}^l(\omega_{up})\ ;\ \mu_j^l = \mu_j^l(\omega_{up});\ \Gamma^l = \Gamma^l(\xi);\ \Delta\psi^l = \Delta\psi^l(\xi) \quad (11)$$

$$U_j = U_j(\omega);\ U_r = U_r(\omega);\ h_j^l = h_j^l(\omega_{up});\ \lambda_j^l = \lambda_j^l(\omega_{up});\ \kappa_r = \kappa_r(\omega);\ \Delta T^l = \Delta T^l(\xi) \quad (12)$$

Under the physical state ω we assume the unification of all state variables (i.e., nonlinear unknowns: pressure, temperature, saturations) of a given control volume. Flux-related fluid properties are defined by the physical state of upstream block ω_{up}, determined at interface l. Next, a state-dependent operator was defined as a function of the physical state only, therefore it is independent of spatial position and represents physical properties of fluids and rock; a space-dependent operator was defined as a function of both physical state ω and spatial coordinate ξ. Then, each term in the Eqs. (3) and (4), with exception for phase source terms, was represented as a product of state-dependent and space-dependent operators. Discretized mass conservation equation reads:

$$a(\xi,\omega)(\alpha_c(\omega) - \alpha_c(\omega_n)) + \sum_l b(\xi,\omega)\beta_c(\omega) + \theta_c(\xi,\omega,u) \quad c = 1, \dots, n_c, = 0, \quad (13)$$

$$a(\xi,\omega) = \phi V\ ;\ \alpha_c(\omega) = \sum_{j=1}^{n_p} x_{cj}\rho_j s_j\ ;\ b(\xi,\omega) = \Delta t\Gamma^l(p^b - p^a);\ \beta_c(\omega) = \sum_{j=1}^{n_p} x_{cj}^l\rho_j^l\frac{k_{rj}^l}{\mu_j^l} \quad (14)$$

Here

- ω, ω_n – state variables on the current and previous timestep respectively,
- u – well control variables,
- p^a, p^b – pressures in blocks a and b connected through interface l.

Discretized energy conservation equation reads:

$$a_e(\xi,\omega)(\alpha_e(\omega) - \alpha_e(\omega_n)) + \sum_l b_e(\xi,\omega)\beta_e(\omega) + \sum_l c_e(\xi,\omega)\gamma_e(\omega) + \theta_e(\xi,\omega,u) = 0, \quad (15)$$

$$a_e(\xi) = V(\xi);\ \alpha_e(\omega) = \phi\left(\sum_{j=1}^{n_p} \rho_j s_j U_j - U_r\right) + U_r;\ b_e(\xi, \omega) = b(\xi, \omega);\ \beta_e(\omega) = \sum_{j=1}^{n_p} h_j^l \rho_j^l \frac{k_{rj}^l}{\mu_j^l}; \tag{16}$$

$$c_e(\xi) = \Delta t \Gamma^l (T^b - T^a);\ \gamma_e(\omega) = \phi\left(\sum_{j=1}^{n_p} s_j \lambda_j - \kappa_r\right) + \kappa_r; \tag{17}$$

Here T^a, T^b are temperatures in blocks a and b connected through interface l. Capillarity and gravity effects are neglected in the existing description of the OBL for simplicity. These effects influence the complexity of flux approximation and should not affect the OBL approach except for the more complex structure of state-dependent operators.

Once these transformations are applied to the governing equations, they identified and distinguished the physical state-dependent operators (α_c, β_c, α_e, β_e, γ_e) in each term of both mass (3) and energy (4) conservation equations. The only exception was made for the source/sink term which can also be processed in a similar manner based on state, space and additional well control variables. Coarsening in physics was achieved by an approximate representation of operators α_c, β_c, α_e, β_e and γ_e within the parameter-space of a simulation problem.

For example, in a binary system with 2 components and 2 phases, which are widely used in geothermic applications, there are only three independent variables in the case of overall molar formulation: pressure p, temperature T and one independent overall composition z. The pressure and temperature ranges are defined by initial and production/injection conditions at wells, while the overall composition is naturally limited by the interval [0,1]. As mentioned above, porosity was added as a pseudo-physical state variable with the corresponding range [0,1]. Next, the interval of each of state variables was divided by the same number m of uniformly distributed points, hereafter referred to as the resolute ion of interpolation table. This resulted in a set of vectors p^m, t^m, z^m and ϕ^m which can be interpreted as the discrete representation of the physical space in a simulation. At the pre-processing stage, operators α_c, β_c, α_e, β_e and γ_e were evaluated at every point of discrete parameter space $\{p^m, t^m, z^m, \phi_0{}^m\}$ and stored in multi-dimensional tables $\alpha_c{}^m$, $\alpha_e{}^m$, $\beta_c{}^m$, $\beta_e{}^m$, $\gamma_e{}^m$. During the course of simulation, the values of state-dependent operators were interpolated along with derivatives for each grid block using created tables. This provided a continuous description based on the interpolation procedure, which accuracy was controlled by the resolution of discretization in the parameter space.

This representation simplifies significantly the implementation of any complex simulation framework. Instead of keeping track of each property and its derivatives with respect to nonlinear unknowns, we can construct an algebraic system of equations with abstract algebraic operators representing the complex physics. The performance of this formulation benefits from the fact that all the expensive evaluations can be done at the pre-processing stage in the limited number of supporting points and are not required in the course of simulation. In addition, the performance of the nonlinear solver is improved since the Jacobian is constructed based on a combination of piece-wise linear operators, which makes system behavior more linear.

3. Numerical results

In this section, we introduce numerical results of simulations based on the described approach. First, in subsection 3.1, we present a three-dimensional heterogeneous model describing a realistic reservoir for low-enthalpy geothermal operations. We show a comparison between simulation using the conventional geothermal formulation in ADGPRS (Wong et al., 2015) and using the COMSOL simulation platform (COMSOL, 2015), which was utilized for a low-enthalpy geothermal simulations in the past (Saeid et al., 2015). COMSOL is an interactive simulation software, where one can model problems from different application fields (e.g., electrical, mechanical, chemical or fluid flow). The penalty of this generality is low computational performance of the simulation.

Further, in subsection 3.2, we display the results of a simple sensitivity analysis of the geothermal model, based on the variation of a doublet position. In subsection 3.3 we present a convergence study of the operator-based linearization for the one-component geothermal model based on different resolutions of parameterized tables using the same reservoir. Finally, similar convergence analysis is performed for a geothermal system with natural gas co-production in low-enthalpy (subsection 3.4) and high-enthalpy (subsection 3.5) regimes.

3.1. Three-dimensional realistic heterogeneous geothermal reservoir

Here, we present the results of a geothermal simulation based on the realistic geological model introduced by Willems et al. (2016). This model is one of the realizations of sedimentological simulation for the Nieuwerkerk sedimentary formation in the West Netherlands Basin. These realizations have been generated for an investigation of performance of a doublet (a pair of injection and production wells) in low-enthalpy geothermal systems. Reservoir dimensions are 1 km × 2 km × 50 m and the discretized model contains 50 × 100 × 20 grid blocks. Both wells are placed in the middle of model, along the long side (Y-axis) with spacing of 1 km; see Fig. 1. The fluvial sandstone bodies are located along the longer side of reservoir, with the porosity distributed within the range [0.16, 0.36] and permeability distributed within the range [6,3360] mD. The boundary conditions along the short (X-axis) of the reservoir are set to a constant initial pressure; the boundary conditions at the other sides are set to no-flow. The reservoir in Fig. 1 is vertically scaled up by a factor of 5 for a better visibility.

Both wells operate under a constant water rate control $q = 2400\ \mathrm{m}^3/\mathrm{day}$. The production well consumes energy from the reservoir, producing hot water at a reservoir temperature $T_{prod} = 348\ \mathrm{K}$. The injection well returns a cold water to the reservoir at $T_{inj} = 308\ \mathrm{K}$, forcing a cold-front propagation to the production well. Both wells are perforated through all layers of the model. Two energy-transfer mechanisms are involved in this process: fluid flow and heat conduction. When the cold front arrives at the production well, temperature drops below a certain limit (338 K in this study) and the so-called doublet lifetime is reached.

To verify the conventional geothermal formulation in the ADGPRS framework, we compare our simulation results with the results of a COMSOL simulation described in Willems et al. (2016). For both simulations, we used similar correlations for properties of fluid and rock described in Saeid et al. (2015). In Fig. 2 we show the comparison between the temperatures at the production well in both cases.

It can be seen that the ADGPRS and COMSOL results are very similar until the time around 50 years when the temperature reduction is already quite significant. These differences can be explained by the differences in the spatial discretization since ADGPRS is using a conservative Finite Volume discretization while COMSOL supports a general Finite-Element discretization. Based on this fact, we believe that the temperature reduction is more realistic in ADGPRS simulation; however, further investigation is required. We use the conventional geothermal formulation by ADGPRS as a reference solution and compare it with the proposed OBL approach.

3.2. Sensitivity analysis of geothermal doublet position

The importance of sensitivity analysis can hardly be overestimated for risk management in geothermal reservoir development. Sometimes key performance indicators dramatically change with a small variation of insignificant parameters. To demonstrate this, we ran a series of geothermal simulations, using the model described above as a base case and varying just one parameter – doublet position. Both wells were

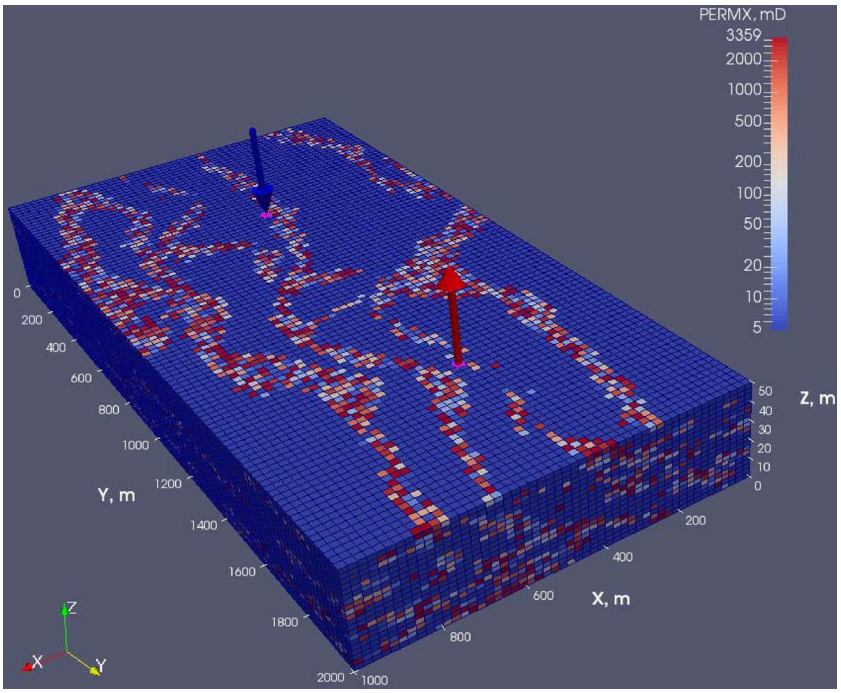

Fig. 1. Permeability distribution and geothermal-doublet configuration of the geothermal reservoir realization used in this paper.

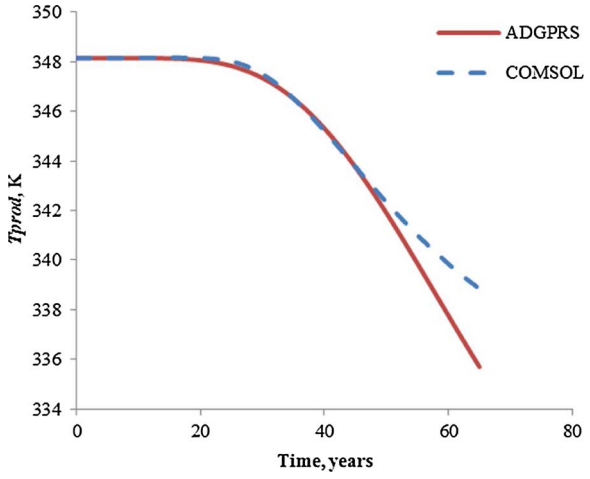

Fig. 2. Comparison between COMSOL and ADGPRS realistic heterogeneous reservoir simulation results.

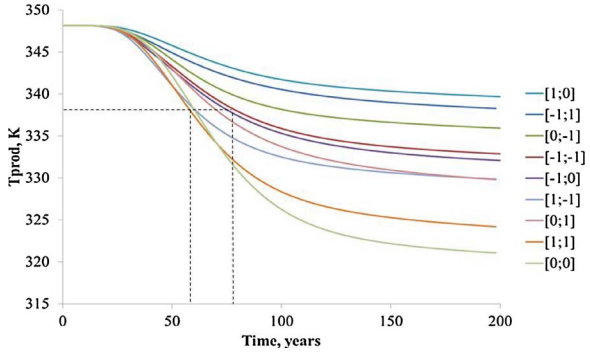

Fig. 3. Variation of the cold-front arrival time for doublet lateral position deviations of one grid cell from the base case [0;0].

simultaneously shifted in lateral direction from the base grid cell to all neighboring cells (including diagonal neighbors), so that their mutual arrangement remained unchanged. Wells were controlled by rate $q = 2400\,\mathrm{m}^3/\mathrm{day}$ during the whole simulation period of 200 years for each of the models. This slight deviation in wells position provoked a large difference in geothermal doublet lifetime (up to 20 years or more, see Fig. 3). The two numbers in square brackets denote the offset (in grid cells) of the doublet position from the base case (denoted as [0;0]) along X and Y axes of the reservoir respectively.

That difference can be explained by different distributions of energy in reservoir, caused by different connectivity between injection and production wells.

Thorough sensitivity and uncertainty analyses help to mitigate reservoir development risks, but require large number of simulations. A tradeoff between number of models to run and available time/computational resources always occurs, that is why the computational performance of reservoir simulation is so important.

3.3. One-component geothermal model

3.3.1. Convergence of operator-based linearization

In this section, we compare the results of simulation for operator-based linearization performed at the different resolutions of interpolation tables and the reference solution based on the conventional linearization method.

We use a simplified variant of the original test case with uniformly distributed thermal properties of rock while rock permeabilities and porosities remain heterogeneous. Both wells work at the same rate control $q = 2400\,\mathrm{m}^3/\mathrm{day}$. Each simulation was performed with a different number of points in the interpolation table which, for simplicity, was equal for all of the unknowns (p, t and φ), while values were uniformly distributed within the range between $p_{min} = 160$ bar and $p_{max} = 250$ bar for pressure, $T_{\min} = 308$ K and $T_{\max} = 349$ K for temperature, and between 0 and 1 for porosity. In order to estimate the error between the reference solution and the solution obtained with operator-based linearization, the following error estimation was introduced:

Table 1
Results of 3D homogeneous simulation.

Resolution	Newton iters.	E_p,%	E_T,%	Linearization cost per Newt.
Std.	174	–	–	1
64	182	0.0005	0.002	0.051
32	212	0.001	0.007	0.054
16	231	0.002	0.028	0.051
8	240	0.008	0.116	0.048
4	245	0.039	0.561	0.051
2	195	0.24	3.775	0.045

$$E = \frac{\sum_{i=0}^{n} |x^i{}_{interp} - x^i{}_{ref}|}{n(\max(x^0{}_{ref},\ldots,x^n{}_{ref}) - \min(x^0{}_{ref},\ldots,x^n{}_{ref}))} \quad (18)$$

Here, n is a number of blocks in the model and x^i is a particular solution value at grid block i. This error was determined at the end of simulation (65 years) for both temperature and pressure variables. The results of comparison are presented in Table 1. The number of points used for interpolation operators is shown in the first column. The second column contains the number of nonlinear iterations, which are directly proportional to the simulation time. The third and fourth columns represent the error in the temperature and pressure solution, respectively. The last column shows relative single average linearization cost (in terms of CPU time) of the new OBL-based simulator prototype with respect to the standard ADGPRS simulator.

From Table 1, the results based on any parameterization approach with resolution of 8 and higher show relatively small error, while the linearization is performed about 20 times faster in comparison with AD-based linearization. At the same time, this cost does not change significantly with an increasing resolution in OBL approach. The error in this simulation is so small because all interpolated properties, based on correlations from Saeid et al. (2015), have substantially linear behavior with respect to the nonlinear unknowns. It seems sufficient in this model to perform the operator-based linearization using the resolution of 8 points. The comparison of the production temperatures and temperature distribution also supports this conclusion, as shown in Fig. 4 and Fig. 5 respectively. Fig. 4 demonstrates a good match between reference and parameterization approach based solution with 8 points, while simulation based on the coarsest table introduces non-physical initial growth of temperature due to a very coarse approximation of operators involved in the energy equation. In Fig. 5, the cold front propagates over the top layer of the reservoir. The top row in Fig. 5 represents the results from the conventional linearization after 15, 30 and 45 years of simulation. The middle row shows the results obtained with OBL using a resolution of 8 points at the same times. The lower row displays absolute difference between the reference and OBL solutions. The injection-well position is marked with the blue circle; the production-well position is shown with the red one.

3.3.2. An analysis of linearization operators

In Fig. 6, we present the most-nonlinear operators used in the proposed linearization approach. All of them are built based on the 64-point interpolation tables in parameter space. These operators correspond to the linearization of mass-accumulation $\alpha_w$and flux β_w terms in the water-component mass equation and energy accumulation α_e and conduction γ_e in the energy equation. They are represented by iso-surfaces in pressure, temperature and porosity parameter space. As expected, all of the operators behave almost linearly in parameter space that explains why the results of simulation with just 8 points are so accurate.

3.4. Two-component low-enthalpy geothermal model

3.4.1. Convergence of operator-based linearization

Here, we demonstrate geothermal simulation with gas co-production using the same three-dimensional reservoir. The injection well injects cold water at $T^w = 308$ K and controlled by a water rate $q^w = 1200\ m^3$/day. The initial reservoir composition of the gas component (methane) $z_1 = 0.1$, with initial pressure $p = 100$ bar, and initial temperature $T = 348$ K. The production well is controlled by the bottom-hole pressure $p^{prod} = 70$ bar. Since the injection rate is now 2

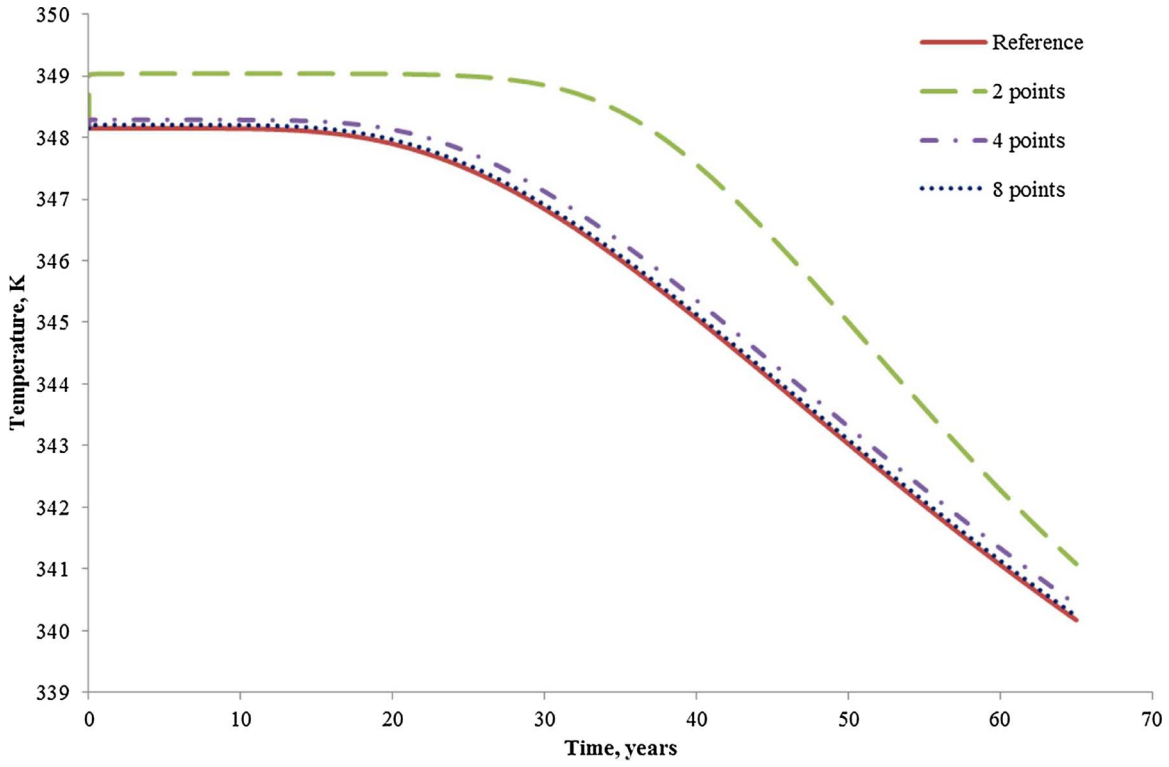

Fig. 4. Comparison of temperatures at production well based on different linearization approaches.

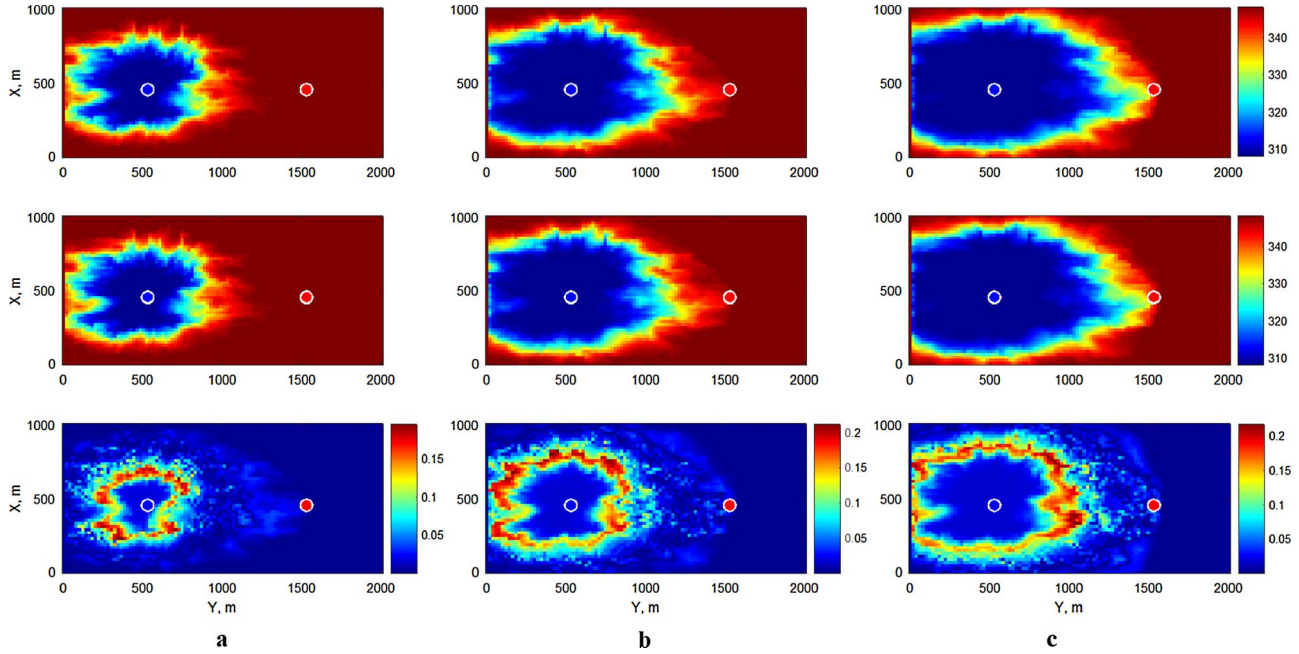

Fig. 5. Temperature front after 15 (a), 30 (b) and 45 (c) years for the conventional linearization (upper), OBL with 8 point resolution (middle), and absolute difference between them (lower) in the top layer of the reservoir.

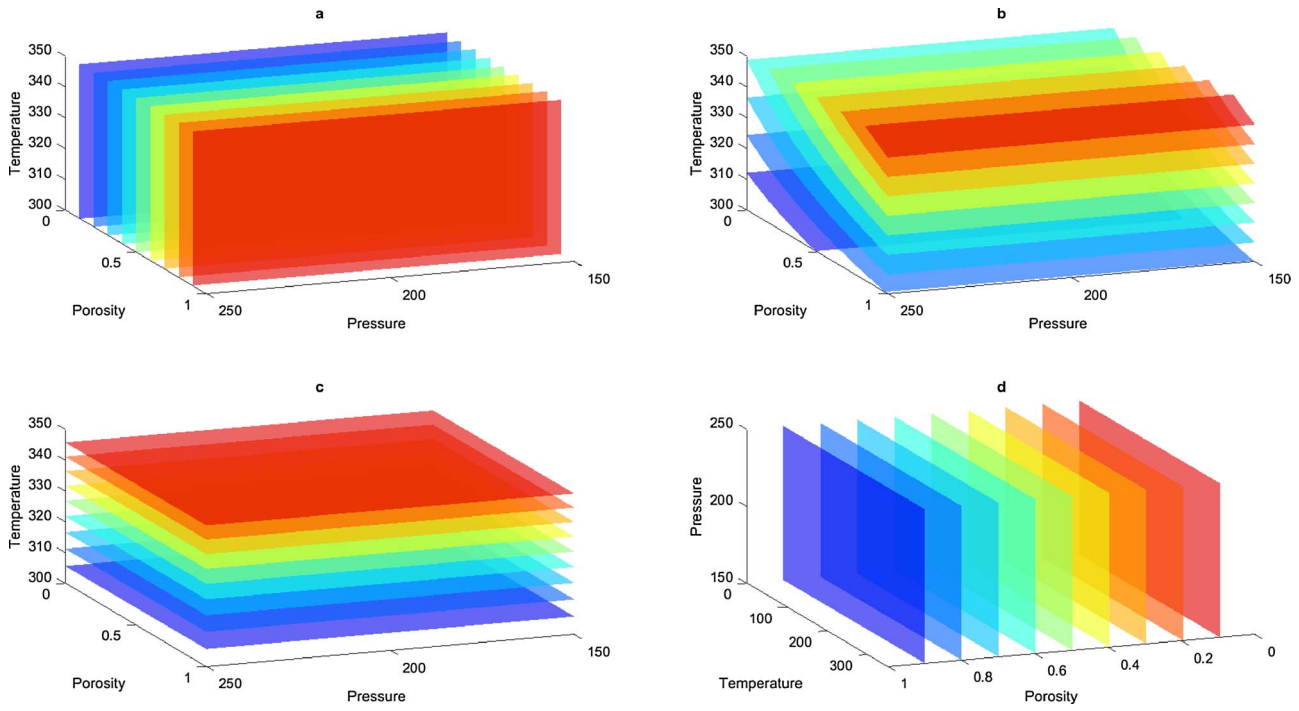

Fig. 6. Physics-based operators of water mass accumulation α_w (a), energy accumulation α_e (b), water mass flux β_w (c) and energy conduction γ_e (d) terms.

times lower, we increased simulation time to 100 years. We used phase behavior and densities based on the Peng-Robinson Equation of State (Peng and Robinson, 1976) with critical parameters described in Table 2. For the enthalpy of the mixture, we used a correlation described in Voskov et al. (2016) with parameters in Table 2. The Lohrenz-Bray-Clark (LBC) correlations was used for the viscosities of each phase (Lohrenz et al., 1964).

We performed a set of simulations with 6 different interpolation-

Table 2
Parameters for properties.

Component	T_c (K)	P_c (bar)	V_c	ACF	M_w	CPG_1	CPG_2	CPG_3	CPG_4
C_1	190.6	46.04	0.098	0.013	16.04	19.251	0.0521	1.197e-5	1.132e-8
H_2O	646.8	220.60	0.056	0.344	18.015	32.243	0.0019	1.055e-5	-3.596e-9

Table 3
Results of 3D, two-phase low-enthalpy simulation.

Resolution	Newton iters.	E_p,%	E_T,%	E_z,%	Linearization cost per Newt.
Std.	1247	–	–	–	1
64	974	0.155	0.809	1.734	0.029
32	968	0.557	1.529	3.692	0.028
16	977	1.305	2.567	6.414	0.028
8	890	1.977	4.288	11.215	0.028
4	890	1.628	5.308	11.397	0.027
2	867	2.191	5.618	13.207	0.027

table resolutions and compared solutions with the reference solution based on the conventional approach. For parameterization, we used uniformly distributed points between $p_{min} = 60$ bar and $p_{max} = 120$ bar for pressure, $T_{\min} = 300$ K and $T_{\max} = 360$ K for temperature, $z_{min} = 0$ and $z_{max} = 1$ for composition, and finally between 0 and 1 for porosity. The results can be seen in Table 3. Columns 1–4 are same as in Table 1, the fifth column shows the error in composition, and the last column shows a relative cost of Operator-Based Linearization per Newton iteration in comparison with AD-based linearization.

The two-component two-phase geothermal model is more challenging for the operator-based linearization approach in comparison to the previous case. However, the error of the OBL method drops significantly with the increasing resolution of interpolation tables. Here, the cost of the Operator-based Linearization is more than 30 times lower in comparison with the AD-based linearization. This happened because in ADGPRS, an iterative solution of EoS is required in the two-phase region, while in OBL, it only required for a limited number of parametrization points. For a higher OBL resolution, the linearization cost insignificantly increases.

Production temperatures for the reference solution and solutions based on linearization operators are shown in Fig. 7. Here, the non-physical behavior for 2-point resolution is similar to the previous case. This behavior is quickly stabilized for the cases with a higher resolution. The comparison of the thermal fronts is shown in Fig. 8. Here, you can see the reference solution (upper row) and the solution based on the OBL with 64 points (middle row) mostly match, and the largest errors of 5 ° are primarily observed around the thermal front. Importantly, the maximum error does not grow along the simulation. Compared to the previous case, the flow is now more influenced by production well because of the changed pressure boundary conditions. Therefore, injected cold water primarily flows towards production well causing faster breakthrough despite lower injection rate.

3.4.2. The analysis of linearization operators

In Fig. 9 we plot 3D isosurfaces to describe the most nonlinear operators in the case of two-phase geothermal model. These operators correspond to the linearization of mass accumulation $\alpha_1$and flux β_1 terms for gas component in the mass equation and energy accumulation α_e and flux β_e in the energy equation. All of the operators are built based on the 64-point interpolation table. They are shown as functions of pressure, temperature and composition at the constant $\varphi = 0.2$. Unlike the pure geothermal case, all operators are highly nonlinear as functions of all state variables.

3.5. Two-component high-enthalpy geothermal model

3.5.1. Convergence of operator-based linearization

Here, we demonstrate geothermal simulation with gas co-production for a high-enthalpy reservoir. The initial temperature, pressure and composition of the gas component (methane) was adjusted to $T = 500$ K, $p = 100$, and $z_1 = 0.1$, which makes the original mixture close to a critical fluid at reservoir conditions. The injection temperature stays the same $T^w = 308$ K, and the injection well operates under a constant water rate control $q = 120\ m^3$/day. Only the top layer of the reservoir was modeled because of the significant reduction in simulation speed. This drop is related to more-expensive phase behavior evaluations (in the near-critical region) for the reference solution and a lower limit of simulation timestep to suppress instabilities associated with high-enthalpy systems (Wong et al., 2016).

Similarly to the previous runs, we performed simulations with 6

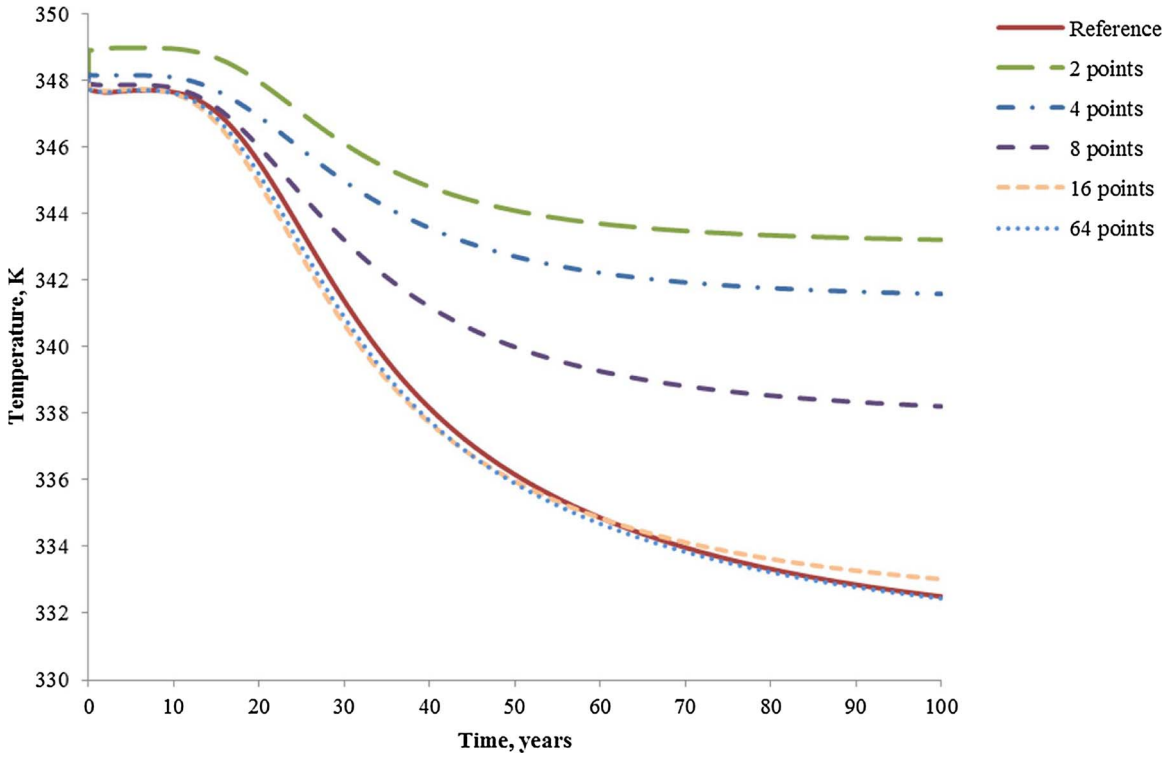

Fig. 7. Comparison of temperatures at production well based on different linearization approaches in low-enthalpy model with co-production.

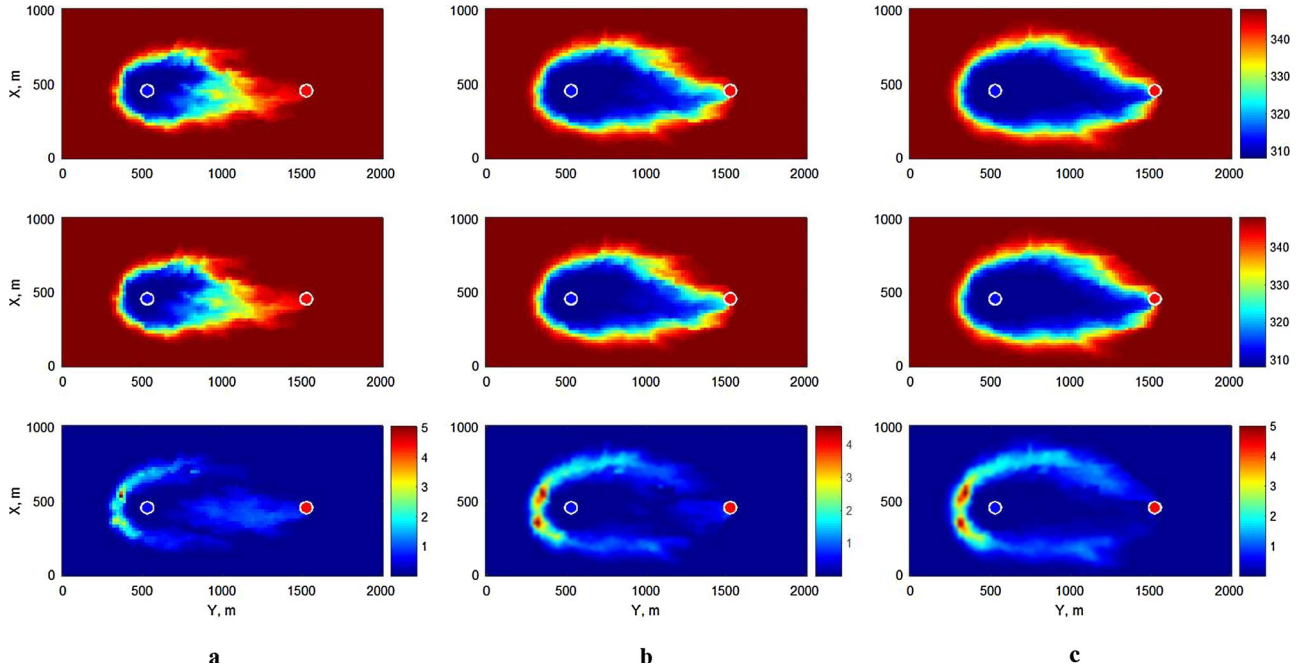

Fig. 8. Temperature front after 20 (a), 40 (b) and 60 (c) years for the conventional linearization (upper), OBL with 64-point resolution (middle), and absolute difference between them (lower) in the top layer of the reservoir in low-enthalpy model with co-production.

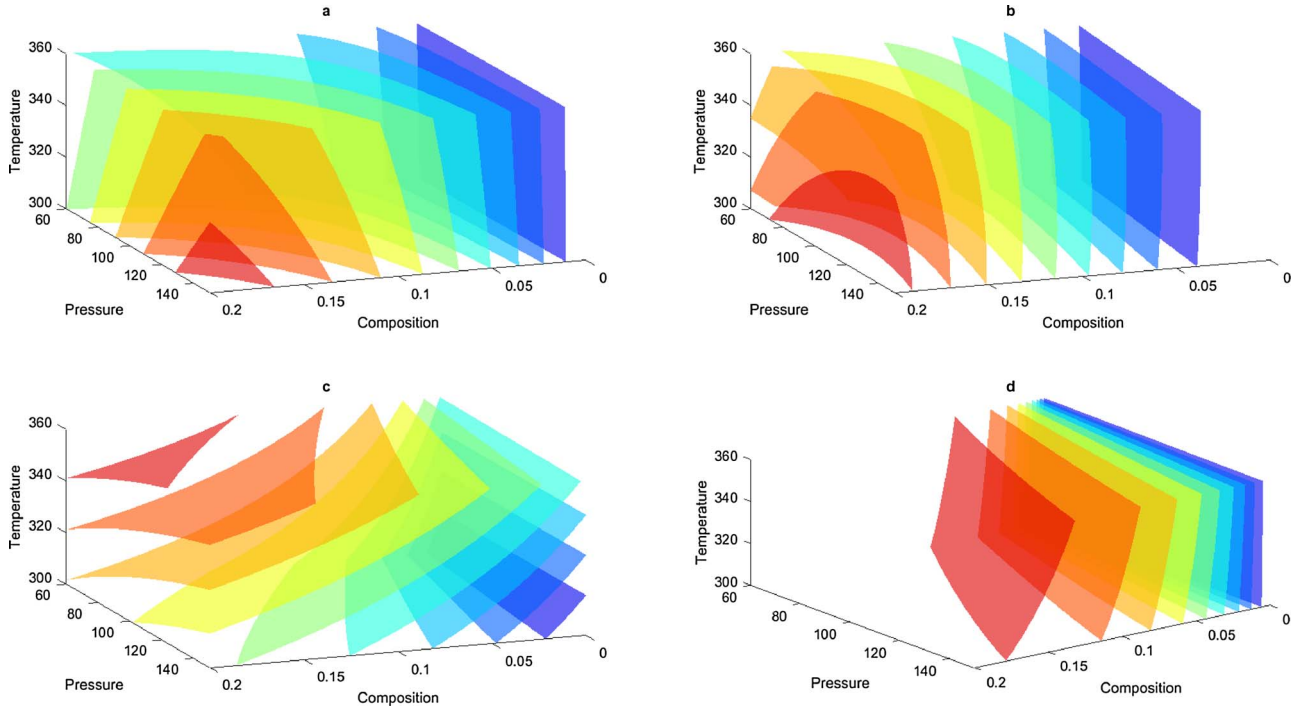

Fig. 9. Physics-based operators of mass accumulation for gas component $\boldsymbol{\alpha}_g$ (a), mass flux for gas component $\boldsymbol{\beta}_g$ (b), energy accumulation $\boldsymbol{\alpha}_e$ (c) and energy flux $\boldsymbol{\beta}_e$ (d) terms in low-enthalpy model with co-production.

resolutions of the interpolation table and compared them with the reference model. For parameterization, we used uniformly distributed points between $p_{min} = 60$ bar and $p_{max} = 290$ bar for pressure, $T_{\min} = 300$ K and $T_{\max} = 510$ K for temperature, $z_{min} = 0$ and $z_{max} = 1$ for composition, and between 0 and 1 for porosity. The results can be seen in Table 4 with columns similar to Table 3.

In comparison to the low-enthalpy case, the high-enthalpy simulation requires much more newton iterations to converge. That is related to the fact that the high-enthalpy system corresponds to more nonlinear pressure-temperature dependencies. However, the operator-based linearization introduces smaller errors, still requiring 64 points to keep the errors below 1%. We believe that overall accuracy increased because the model has become 2-dimensional, therefore some factors affecting the solution, such as vertical conduction, are no longer present. Still, the error of the operator-based linearization decreases as the resolution of interpolation tables. The cost of linearization per Newton iteration behaves similarly to the low-enthalpy case.

Production temperatures for the reference solution and solutions based on the linearization operator are shown in Fig. 10. The lowest resolution in the physical tables introduces a large error in the

Table 4
Results of 2D two-phase high-enthalpy simulation.

Resolution	Newton iters.	E_p,%	E_T,%	E_z,%	Linearization cost per Newt.
Std.	7617	–	–	–	1
64	2715	0.023	0.092	0.711	0.027
32	2629	0.071	0.356	2.257	0.027
16	2489	0.096	0.496	3.443	0.026
8	2118	0.07	0.615	3.748	0.026
4	2113	0.088	1.104	3.99	0.027
2	1901	0.108	4.279	3.672	0.026

temperature breakthrough time, as it was expected from Table 4. With higher resolutions, the behavior becomes closer to the reference solution, even though some non-physical oscillations can be observed at intermediate resolutions, e.g. 4-point resolution in Fig. 10. The spatial distribution of temperature demonstrates certain discrepancy between two approaches – up to 2°, as it can be seen in Fig. 11. As in previous cases, the maximum error does not increase along the simulation and concentrated around the thermal front.

3.5.2. *The analysis of linearization operators*

In Fig. 12, we plot again 3D isosurfaces to describe operators in the case of a high-enthalpy geothermal model with co-production. Here we show the same operators as in Fig. 9. For the high-enthalpy case all operators demonstrate more nonlinear behavior. That is partially due to the closeness to superheated conditions of the gas-water mixture and partially due to the larger interval of changes in temperature covered in simulations. We hope that in the future work, the detailed analysis of parametrized operators will help to improve the nonlinear solver in geothermal simulations.

4. Conclusions

In this paper, we demonstrate the applicability of the operator-based linearization approach to the simulation of thermal multi-component, multiphase flow in porous media. Both mass- and energy-conservation equations were transformed to an operator form where each term was represented as the product of state-dependent and space-dependent operators. During the pre-processing stage, all state-dependent operators were discretized in the parameter space of the simulation problem and introduced as a set of interpolation tables. In the course of a simulation, these operators were updated based on multi-linear interpolation, while the rest of the equation terms were computed using the conventional approach. The operator-based linearization was applied to a geothermal system with gas co-production where pressure, temperature, composition and initial porosity were used as state parameters. The addition of porosity to the state variables helps to reduce the number of state-dependent operators. A similar approach can be used to handle the changes in mass of solid phase(s) due to the chemical precipitation and dissolution.

We used a realistic reservoir model of a low-enthalpy geothermal doublet to test the approach. Simulation results showed that proposed approach can reproduce the reference solution results quite accurately with a reasonable resolution of interpolation tables. For a single-component low-enthalpy geothermal model, a relatively coarse resolution of interpolation tables was able to handle all governing nonlinearities and matched the reference solution based on full physics almost precisely. For a two-component geothermal model with natural gas co-production, the required resolution of interpolation tables was higher. This happened due to the highly-nonlinear nature of linearization operators in case of two-phase systems. However, the simulation with a coarser resolution still can be used as fast proxy models in the inversion and uncertainty quantification process. It is important to notice that the proposed linearization approach significantly improves the performance of linearization in comparison with the AD-based linearization. The relative cost of Operator-Based Linearization does not grow significantly with the increased resolution while the number of nonlinear iteration is decreasing with coarser representation.

The extended approach described in this paper substantially simplifies the assembly of the residual and Jacobian in nonlinear solution. At the same time, the operator-based version of the original problem could be seen as a proxy model, where the accuracy of the nonlinear

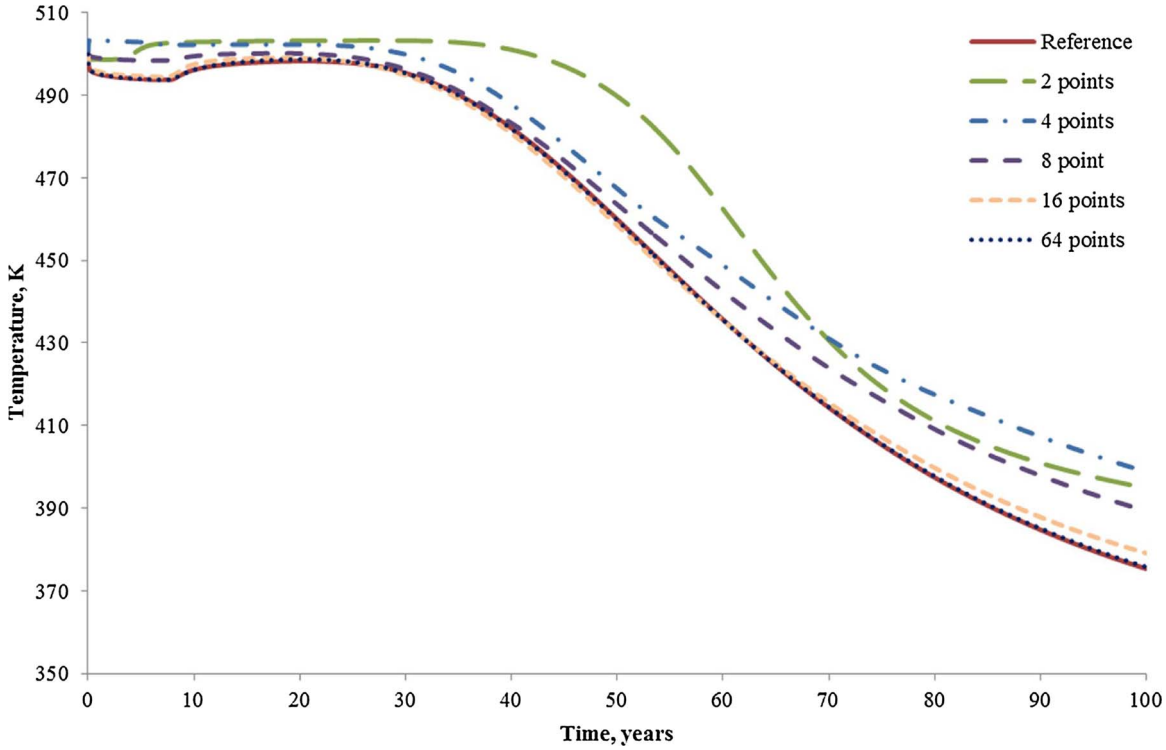

Fig. 10. Comparison of temperatures at production well based on different linearization approaches in the high-enthalpy model with co-production.

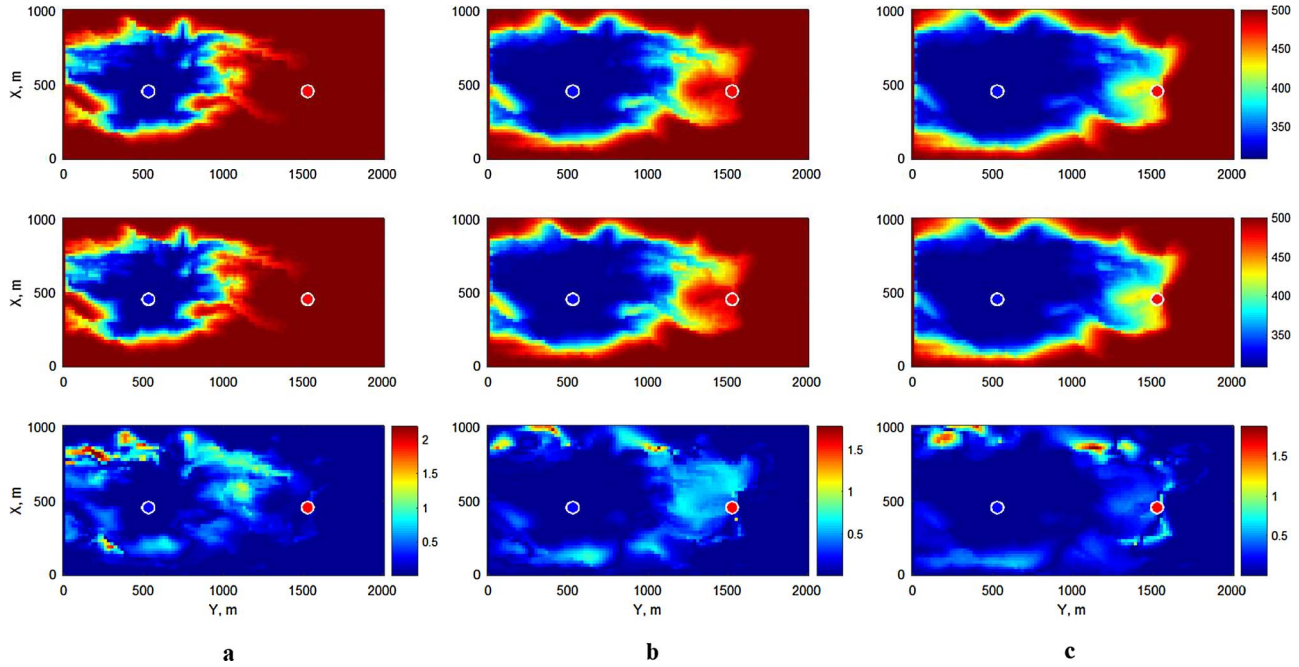

Fig. 11. Temperature (condensation) front after 20 (a), 40 (b), and 60 (c) years for the conventional linearization (upper), OBL with 64-point resolution (middle), and absolute difference between them (lower) in high-enthalpy model with co-production.

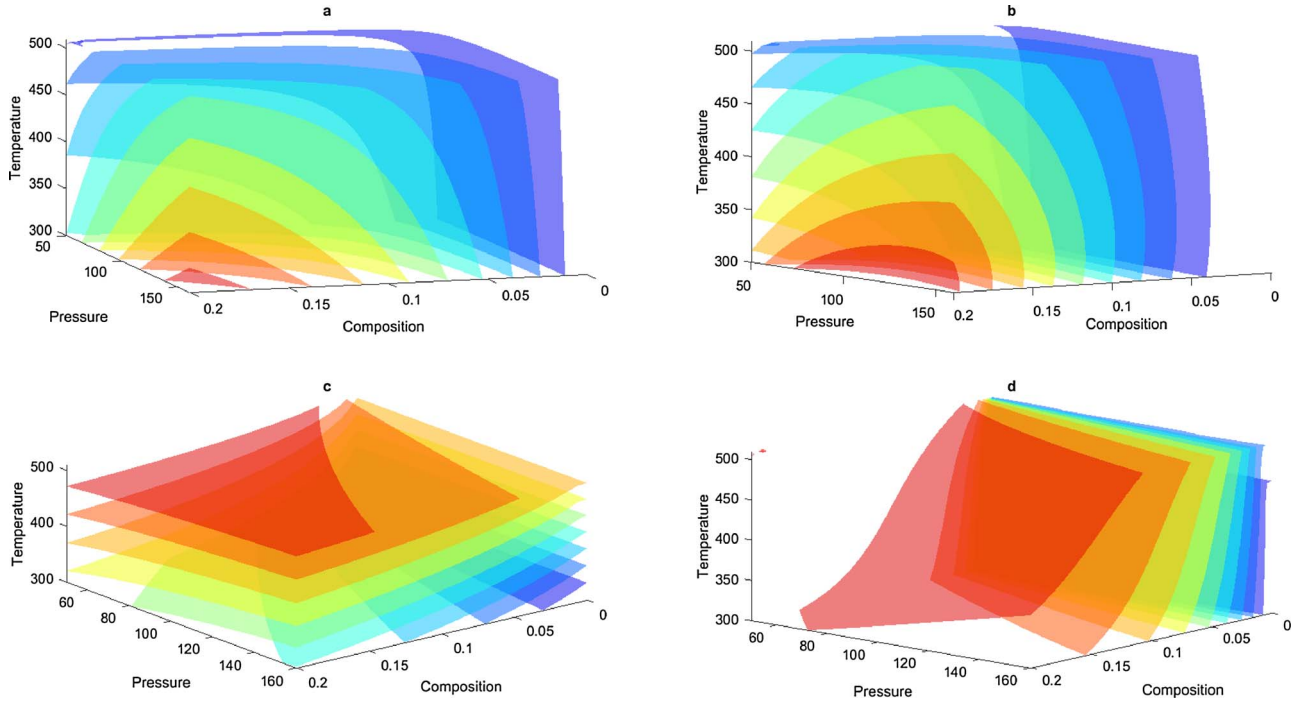

Fig. 12. Physics-based operators of mass accumulation for gas component $\boldsymbol{\alpha}_g$ (a), mass flux for gas component $\boldsymbol{\beta}_g$ (b), energy accumulation $\boldsymbol{\alpha}_e$ (c) and energy flux $\boldsymbol{\beta}_e$ (d) terms in high-enthalpy model with co-production.

representation of the physics can be balanced with the performance of the nonlinear solver. Here we used the most-straightforward approach and defined the parameter space of the problem explicitly in a uniform fashion. For reservoir simulation, an adaptive parametrization in parameter space seems more attractive both in terms of efficiency and memory management. The combination of the adaptive parametrization and coarsening in physical space based on a simple error estimator provides an excellent opportunity for nonlinear analysis, which is a crucial requirement for high-enthalpy systems. Finally, the simplicity of the Jacobian assembly in the new approach helps to transfer the geothermal simulation code to emerging architectures and significantly improve the performance. As the result, the proposed simulation approach will open new opportunities for inverse modeling, optimization and risk analysis for practical geothermal applications.

References

Aziz, Khalid, Settari, Antonin, 1979. Petroleum Reservoir Simulation. Chapman & Hall.
COMSOL Multiphysics Reference Manual, 5.1.
Collins, D., Nghiem, L., Li, Y.K., Grabenstetter, J., 1992. Efficient approach to adaptive-implicit compositional simulation with an equation of state. SPEJ 7 (2), 259–264.

Geoquest, 2011. Eclipse technical description. Schlumberger 2.
Iranshahr, A., Voskov, D., Tchelepi, H.A., 2010. Generalized negative-flash method for multiphase multicomponent systems. Fluid Phase Equilib. 299 (2), 272–284. http://dx.doi.org/10.1016/j.fluid.2010.09.022.
Iranshahr, A., Voskov, D.V., Tchelepi, H.A., 2013. Tie-simplex based compositional space parameterization: continuity and generalization to multiphase systems. AIChE J. 59, 1684–1701.
Khait, M., Voskov, D.V., 2017a. Operator-based linearization for general purpose reservoir simulation. J. Petrol. Sci. Eng. 157, 990–998.
Khait, M., Voskov, D., 2017b. GPU-offloaded general purpose simulator for multiphase flow in porous media. Soc. Petrol. Eng. http://dx.doi.org/10.2118/182663-MS. SPE Reservoir Simulation Conference.
Lohrenz, J., Bray, B.G., Clark, C.R., 1964. Calculating viscosities of reservoir fluids from their compositions, SPE paper 915. J. Petrol. Technol. 1171–1176.
Lucia, A., Padmanabhan, L., Venkataraman, S., 2000. Multiphase equilibrium flash calculations. Comput. Chem. Eng. 24 (12), 2557–2569.
Noy, D., Holloway, S., Chadwick, R., Williams, J., Hannis, S., Lahann, R., 2012. Modelling large-scale carbon dioxide injection into the bunter sandstone in the UK southern north sea. Int. J. Greenh. Gas Control 9, 220–233.
O'Sullivan, J., Croucher, A., Yeh, A., O'Sullivan, M., 2014. Further improvements in the convergence of tough2 simulations (2014) 11th world congress on computational mechanics, WCCM 2014. In: 5th European Conference on Computational Mechanics, ECCM 2014 and 6th European Conference on Computational Fluid Dynamics. ECFD. pp. 5929–5940.
Peng, D.-Y., Robinson, D.B., 1976. A new two-Constant equation of state. Ind. Eng. Chem. Fundam. 15, 59–64.
Pruess, K., 2006. Enhanced geothermal systems (EGS) using CO2 as working fluid-A novel approach for generating renewable energy with simultaneous sequestration of carbon. Geothermics 35 (4), 351–367.
Saeid, S., Al-Khoury, R., Nick, H.M., Hicks, M.A., 2015. A prototype design model for deep low-enthalpy hydrothermal systems. Renew. Energy 77, 408–422.
Vanden, K.J., Orkwis, P.D., 1996. Comparison of numerical and analytical Jacobians. AIAA J. 34 (6), 1125–1129.
Voskov, D.V., Tchelepi, H.A., 2012. Comparison of nonlinear formulations for two-phase multi-component EoS based simulation. J. Petrol. Sci. Eng. 82, 101–111.
Voskov, D.V., 2011. An extended natural variable formulation for compositional simulation based on tie-line parameterization. Transp. Porous Media 86.
Voskov, D.V., 2017. Operator-based linearization approach for modeling of multiphase multi-component flow in porous media. J. Comput. Phys. 337, 275–288.
Voskov, D., Zaydullin, R., Lucia, A., 2016. Heavy oil recovery efficiency using SAGD, SAGD with propane co-injection and STRIP-SAGD. Comput. Chem. Eng. 88, 115–125. http://dx.doi.org/10.1016/j.compchemeng.2016.02.010.
Willems, C.J.L., Goense, T., Nick, H.M., Bruhn, D.F., 2016. The relation between well spacing and net present value in fluvial hot sedimentary aquifers; a west Netherlands basin case study. In: Proceedings, 41 st Workshop on Geothermal Reservoir Engineering. Stanford University, Stanford, CA. . https://pangea.stanford.edu/ERE/db/GeoConf/papers/SGW/2016/Willems.pdf.
Wong, Z.Y., Horne, R., Voskov, D., 2015. A geothermal reservoir simulator in AD-GPRS. Proceedings World Geothermal Congress. https://pangea.stanford.edu/ERE/db/WGC/papers/WGC/2015/22043.pdf.
Wong, Z.Y., Horne, R., Voskov, D., 2016. Comparison of nonlinear formulations for geothermal reservoir simulations. 41 st Workshop on Geothermal Reservoir Engineering. . https://pangea.stanford.edu/ERE/db/GeoConf/papers/SGW/2016/Wong.pdf.
Zaydullin, R., Voskov, D.V., Tchelepi, H.A., 2013. Nonlinear formulation based on an equation-of-state free method for compositional flow simulation. SPE J. 18 (2), 264–273.
Zaydullin, R., Voskov, D., James, S., Lucia, A., 2014. Fully compositional and thermal reservoir simulation. Comput. Chem. Eng. 63, 51–65.